ISSN　2435-5453

# Technical Journal of Advanced Mobility

## 次世代移動体技術誌

## 巻 頭 言



## 論　文



JUADA
Japan UAS Industrial Development Association

Vol. 7
2026

# フィジカル AI ドローンのジャーナル

テクニカルジャーナル編集委員長
一般社団法人日本 UAS 産業振興協議会
常務理事　岩田　拡也

2026 年が幕を開けました。謹んで新年のご挨拶を申し上げます。

一般社団法人日本UAS産業振興協議会(JUIDA)が発行するTechnical Journal of Advanced Mobility(TJAM)は、ドローン産業の振興に役立つ技術情報を産業界の皆様に提供するために創設されたオンライン技術情報誌で、掲載論文は年々増加を続けております。毎年進化を続ける TJAM ですが、昨年 2025 年も例えば、Letter で一度発表した後、正式に論文で再投稿されるパターンや、英語版と日本版（母国語版）の両方掲載できる新しい制度を活用する著者も出て参りました。今後は世界のドローンおよびエアモビリティ関係者に読んで頂けるジャーナルを目指して参ります。その一環として 2026 年から巻頭言も英語版をご用意することとなりました。今後とも TJAM をグローバルに活用して頂ければ幸いです。

そのグローバルの話題ですが、毎年多くの国々の参加で活況を呈している Japan Drone 展で、2026 年もポスターセッション開催が決定しております。今年もプレゼンコーナーをご用意しておりますので、若手研究者や学生の在籍する研究室からのご参加をお待ちしております。また Japan Drone のポスターセッションは、学術論文でオーサービジットが可能な貴重な機会ですので、今年も著者に集まっていただけるような場を検討しております。本ジャーナルの著者は産業界や学術界など多岐に渡る分野の方々ですので、産官学一体となって情報交換や情報共有を促進するエコシステムの役割も TJAM は果たします。この役割は国境を越えてグローバルに存在しますので、海外からの投稿も積極的に募集していきたいと考えております。

今年 2026 年は、世界が大きく変革する節目と目されていて、FAA のパート 108 の高度に自動化した目視外飛行など先進的な空の技術と向き合いチャレンジするまさに「天馬行空」の年です。下水管内を点検するマイクロドローンから、数千機同時飛行するドローンショー、成層圏に浮かぶ巨大な HAPS 型宇宙光通信６G ドローンまで、無人航空機やエアモビリティの技術は多様化しています。TJAM は、その多様な新技術の発展と情報共有に貢献して参ります。本年も何卒宜しくお願い申し上げます。

2026 年 1 月吉日

岩田　拡也 Kakuya Iwata

国立研究開発法人 産業技術総合研究所上級主任研究員。1998 年通商産業省工業技術院 電子技術総合研究所に入所。第 16 回電子材料シンポジウム EMS 賞受賞。第 12 回応用物理学会講演奨励賞受賞。青色 LED 開発、半導体製造装置開発から産業用飛行ロボット開発に至り、2007 年日本機械学会交通・物流部門優秀講演表彰を受賞。2008 年に経済産業省 製造産業局 産業機械課にてロボット政策に従事。2009 年以降「NIIGATA SKY PROJECT」の無人航空機開発を立ち上げ、2014 年に JUIDA 設立。2018 年より ISO TC 20/SC 16(無人航空機)に参加し、2022 年経済産業省 産業標準化事業表彰受賞、日本品質管理学会第 52 回年次大会研究発表会優秀発表賞受賞。

Foreword: 'The Journal for Physical AI Drones'
Chairman of the Technical Journal Editorial Committee
Japan UAS Industrial Development Association (JUIDA)
Executive Director Kakuya Iwata

The year 2026 has commenced. We extend our sincere New Year's greetings.
The Technical Journal of Advanced Mobility (TJAM), published by the Japan UAS Industrial Development Association (JUIDA), is an online technical information magazine established to provide industry stakeholders with technical information beneficial to the advancement of the drone industry. The number of papers published continues to increase year by year. While the Technical Journal continues to evolve annually, last year (2025) saw new patterns emerge. For instance, authors first published a Letter before formally resubmitting it into a full paper, and some utilized the new system allowing simultaneous publication in both English and Japanese (native language) editions. Moving forward, we aim to develop the journal into one accessible to drone and air mobility professionals worldwide. As part of this effort, from 2026, the opening statement will also be available in English. We would be delighted if TJAM continues to be utilized by readers around the world.
Regarding global engagement, the poster session at Japan Drone, which sees lively participation from many countries each year, has been scheduled for 2026. We will again provide a presentation corner and look forward to participation from laboratories with young researchers and students. Furthermore, the Japan Drone poster session offers a valuable opportunity for author visits based on academic papers, so we are considering ways to encourage authors to gather there again this year. As authors of this journal span diverse fields including industry and academia, TJAM also serves as an ecosystem promoting information exchange and sharing across industry, government, and academia. This role extends globally beyond national borders, so we actively encourage submissions from overseas.

The year 2026 is viewed as a pivotal moment of significant global transformation. It is truly a year of boundless imagination, confronting and challenging advanced aerial technologies such as the highly automated beyond visual line of sight (BVLOS) flights under FAA Part 108 regulations. From micro-drones inspecting sewer pipes to drone shows involving thousands flying simultaneously, and even massive HAPS-type space optical communication 6G drones floating in the stratosphere, unmanned aerial vehicle and air mobility technologies are diversifying. TJAM will contribute to the development and information sharing of these diverse new technologies. We look forward to your continued support this year.

January 2026

**Kakuya Iwata**
Senior Principal Researcher, National Institute of Advanced Industrial Science and Technology (AIST). Joined the Electronics and Telecommunications Research Institute, Agency of Industrial Science and Technology, Ministry of International Trade and Industry (MITI) in 1998. Recipient of the 16th Electronic Materials Symposium EMS Award. Recipient of the 12th Applied Physics Society Presentation Encouragement Award. His work spans from blue LED development and semiconductor production equipment development to industrial flying robot development. Received the 2007 Japan Society of Mechanical Engineers Transportation and Logistics Division Outstanding Presentation Award. Engaged in robot policy at the Industrial Machinery Division, Manufacturing Industries Bureau, Ministry of Economy, Trade and Industry in 2008. Launched the unmanned aircraft development for the "NIIGATA SKY PROJECT" in 2009, establishing JUIDA in 2014. Served as an ISO TC20/SC16 (Unmanned Aircraft Systems) expert since 2018. Received the Ministry of Economy, Trade and Industry Industrial Standardization Project Award in 2022 and the Excellent Presentation Award at the 52nd Annual Conference Research Presentation Session of the Japan Society for Quality Control in 2022.

# Development of $CO_2$ Gas Sensing Method using Formation Flight with Four Drones

Shanfeng Zhang[*1], Shigenori Togashi[*2], Etsuki Yoshimura[*2]
Graduate School of Advanced Science and Engineering, Waseda University[*1]
Mechanical Engineering Course, School of Science and Engineering, Kokushikan University[*2]

Understanding gas concentration distributions near the ground is important for disaster prevention and safety management. In this study, as part of expanding drone applications, we tried to develop the $CO_2$ gas sensing method using formation flight with four drones. By flow simulation, we confirmed the gas updraft flow not only velocity but also concentration distribution generated by the drones. It was confirmed that the updraft flow velocity around the sensor was 2 m/s at the height of 0.3 m, and the concentration ratio was between 0.95 and 0.99, respectively. Then, to stable the formation flight with four drones, a rope was used between the connecting rod and the drone. Then, the $CO_2$ sensing experiment using this approach was conducted. The average concentration values of 4,290 and 4,710 ppm of three experiments were measured at the heights of 0.5 m and 0.3 m, respectively. Moreover, we tried to predict the concentration at the $CO_2$ source using the steady-state one-dimensional convection-diffusion equation. It was found that the predicted concentration of 4,772 ppm at the $CO_2$ source was in between 4,700 and 4,800 ppm measured by sensor. Finally, the effectiveness of prediction was confirmed.

***Keywords:*** Drone, Formation flight, Flow simulation, Gas sensing, Convection, Diffusion, Prediction

## 1. Introduction

There is a wide range of possible applications for drones, such as for infrastructure inspection, agriculture, logistics, photography, disaster prevention, and gas sensing. In dangerous site inspection, their ability to quickly collect information in hazardous areas where human entry is dangerous has become increasingly important. The poisonous hydrogen sulfide ($H_2S$) gas and high concentration $CO_2$ gas, being heavier than air, tend to accumulate near the ground in underground or enclosed spaces, potentially causing delayed responses, oxygen deficiency, or poisoning. Understanding gas concentration distributions in such environments is important for disaster prevention and safety management. In recent years, papers have been published on the use of drones for gas sensing tasks. Li, et al. [1] reported the air quality monitoring, and Motlagh, et al. [2] reported the air pollution monitoring using a drone in flight, respectively. On the other hand, Neumann, et al. [3] reported results of gas source localization experiments using a drone equipped with several different types of gas sensors by applying a particle filter-based algorithm to the sensor data collected in flight. Successful gas source localization demonstrations were also reported for a drone equipped with a laser-based remote methane detector [4]. Despite these successful examples, there is a problem using drone for gas sensing tasks. The rotors of a drone produce a strong downwash to obtain the lift force. Most gas sensors show a response only when a gaseous chemical substance touches the sensor surface. The gas contained in the surrounding air needs to be transported to the sensor surface by convection and diffusion. When a drone flies, the downwash generated by rotors blows off the gas near the ground. This problem has been raised even in early work on gas sensing drones [5]. To solve the above problem, Sato, et al. [6] proposed the gas sensing method by using the fountain flow [7] generated by the two drones connected by a rod. In their paper, the flow velocity distribution by numerical simulation and the experimental results with air were also reported. Moreover, Akaogi, et al. [8] proposed the gas sensing method by using the fountain flow generated by the extended arm quad type drone. In their paper, their experimental results with ethanol gas were also reported.

In the above previous studies, there are still some issues as follows. First, the gas updraft flow velocity distribution generated by the drones is shown using flow simulation, but the gas concentration distribution is not shown. Second, the formation flight equipped with the gas sensor is unstable in case of direct connection between rods and each drone. Third, there was no prediction of $CO_2$ concentration at the source based on the sensing point.

Therefore, in this study, we assumed the application example of $CO_2$ sensing with heavier than air and larger amount at the underground parking lot as shown in **Fig.1**. First, flow simulation was conducted to visualize the gas updraft flow not only flow velocity but also concentration distribution generated by the drones as detailed in Chapter 2. Second, the formation flight equipped with the gas sensor is unstable in case of direct connection between rods and each drone. Therefore, a rope was used between the connecting rod and the drone, instead of connecting the rod directly to the drone. With this approach, the individual differences of drone position and height were compensated for by the rope, and the formation flight with four drones were stably continued as detailed in Chapters 3 and 4. Third, we conducted $CO_2$ sensing experiments using formation flight with four drones and predicted $CO_2$ concentration at the source from the sensing points using the one-dimensional convection-diffusion equation as detailed in Chapters 5, 6, and 7.

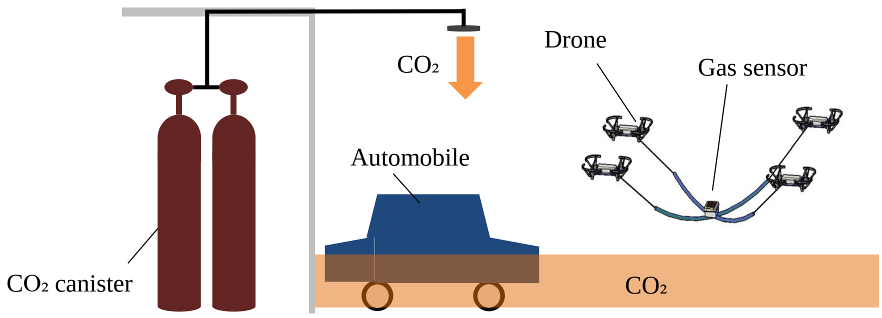


**Fig.1** Application example of $CO_2$ sensing at the underground parking lot.

## 2. Flow simulation

To visualize the gas updraft flow not only flow velocity but also concentration distribution generated with the drones, flow simulation was conducted using the software Flowsquare$^+$ [9-11]. The gas concentration transport equation is also solved with the momentum transport equation in Flowsquare$^+$, and the application example papers have been published [12,13]. **Figure 2** shows the flow simulation domain and boundary conditions of flow simulation around two drones. Parameters $lx$, $ly$, $lz$, $nx$, $ny$, and $nz$ represent Length in x, y, z direction, number of grids in x, y, and z direction, respectively. **Table 1** is specification of parameters using the boundary conditions of flow simulation. Here, the domain in the z direction was thinned to perform quasi-two-dimensional simulation. Parameters $W_d$, $P_d$, and $H_d$ represent the width of drone, the diameter of drone propeller, and hovering height, respectively. Flow simulation conducted both one drone and two drones. In case of two drones, $L$ represents the distance between drones as shown in **Fig.2**. Parameters $V$inG and $V$inR are the inflow velocity at the top of drone propeller (Boundary color: Green) and the outflow velocity at the bottom of drone propeller (Boundary color: Red) measured with a Pitot tube and set to 8 m/s as the velocity boundary condition of drone

1. Similar boundary conditions were also set for drone 2. Parameters $W_s$, $H_s$, and $D_s$ represent the width of sensor housing, installation height of sensor housing, and thickness of sensor housing, respectively. Here, the sensor housing was set only in case of simulation for two drones.

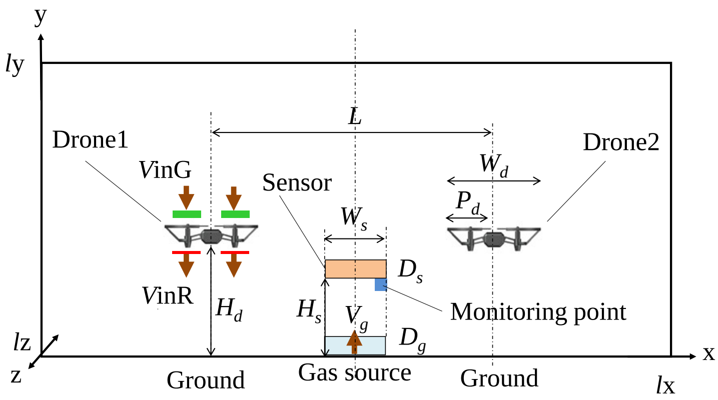


**Fig.2** Flow simulation domain and boundary conditions.

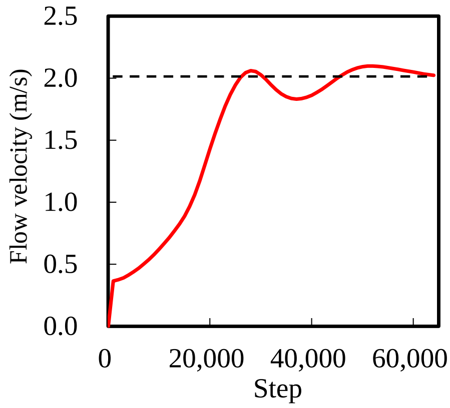


**Fig.3** Flow velocity convergence at the monitoring point.

**Table 1** Specification of parameters using the boundary conditions of flow simulation.

| No. | Parameters | Explanation of parameters | Input data | |
|---|---|---|---|---|
| | | | One drone | Two drones |
| 1 | *l*x | Length in x direction (m) | 2.5 | 2.5 |
| 2 | *l*y | Length in y direction (m) | 1.0 | 1.0 |
| 3 | *lz* | Length in z direction (m) | 0.05 | 0.05 |
| 4 | *n*x | Number of grids in x direction | 250 | 250 |
| 5 | *n*y | Number of grids in y direction | 100 | 100 |
| 6 | *nz* | Number of grids in z direction | 5 | 5 |
| 7 | $W_d$ | Width of drone (m) | 0.20 | 0.20 |
| 8 | $P_d$ | Diameter of drone propeller (m) | 0.08 | 0.08 |
| 9 | $H_d$ | Hovering height (m) | 0.4 | 0.4 |
| 10 | $L$ | Distance between drones (m) | - | 1.5 |
| 11 | *V*inG | Inflow velocity at the top of drone propeller (Boundary color: Green) | -8.0 | -8.0 |
| 12 | *V*inR | Outflow velocity at the bottom of drone propeller (Boundary color: Red) | -8.0 | -8.0 |
| 13 | $W_s$ | Width of sensor housing (m) | - | 0.2 |
| 14 | $H_s$ | Installation height of sensor housing (m) | - | 0.3 |
| 15 | $D_s$ | Thickness of sensor housing (m) | - | 0.05 |
| 16 | $D_g$ | Thickness of gas ejection source (m) | - | 0.05 |
| 17 | $V_g$ | Gas ejection velocity (m/s) | 0.1 | 0.1 |
| 18 | $C_g$ | Gas concentration ratio | 1.0 | 1.0 |
| 19 | *mu* | Air viscosity coefficient (Pa·s) | $1.8\times10^{-5}$ | $1.8\times10^{-5}$ |
| 20 | $C_s$ | Coefficient of Smagorinsky turbulence model | 0.17 | 0.17 |
| 21 | *cfl* | Courant-Friedrichs-Lewy number | 0.01 | 0.01 |

Parameters $D_g$, $V_g$, and $C_g$ represent the thickness of gas ejection source, gas ejection velocity, and gas concentration ratio, respectively. Last parameters *mu*, $C_s$, and *cfl* represent air viscosity coefficient, the coefficient of Smagorinsky turbulence model [14,15], and Courant-Friedrichs-Lewy number, respectively. For stable flow simulation, the Courant number (CFL) number for the explicit method was set to a small value of 0.01. **Figure 3** shows the state of flow velocity convergence at the monitoring point near the sensor in **Fig.2**. It was confirmed that the flow velocity at the monitoring point converged to approximately 2.0 m/s after 63,000 simulation steps.

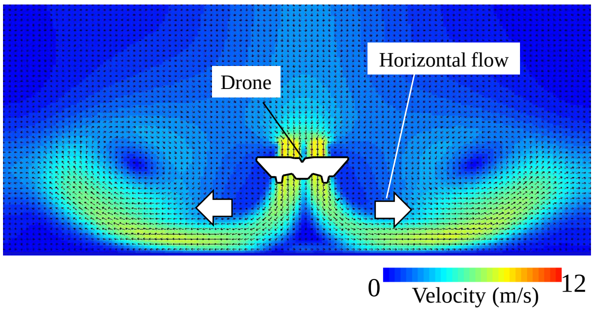


(a) Flow velocity distribution

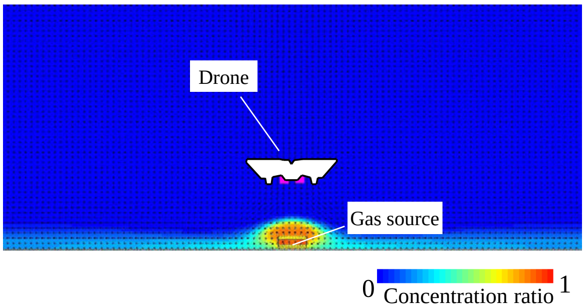


(b) Concentration distribution

Fig.4 Flow simulation results in case of one drone.

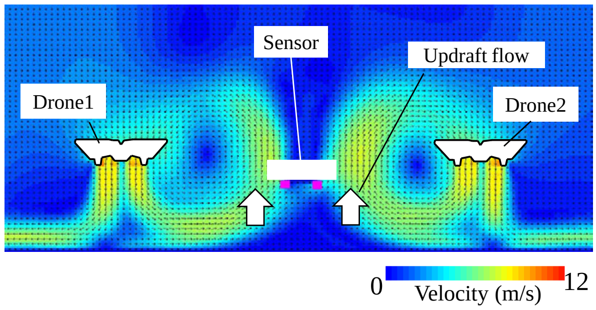


(a) Flow velocity distribution

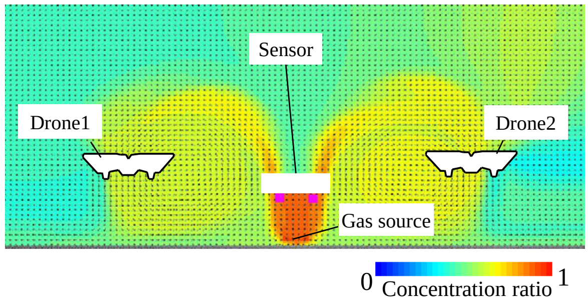


(b) Concentration distribution

Fig.5 Flow simulation results in case of two drones.

Figure 4 shows the flow simulation results in case of one drone. Figures 4(a) and 4(b) are the flow velocity and concentration distribution, respectively. The downwash flow generated by the drone spread out as the horizontal flow along the ground after reaching the ground as shown in Fig.4(a). Therefore, it has been confirmed that the concentration distribution from the gas source became horizontally as shown in Fig.4(b). Here, the concentration distribution is expressed as the normalized concentration ratio and ranges from 0 to 1.

Figure 5 shows the flow simulation results in case of two drones. Figures 5(a) and 5(b) are the flow velocity and concentration distribution, respectively. The downwash flow generated by two drones rolled up as the updraft flow after reaching the ground. Therefore, it has been confirmed that the concentration from the gas source became updraft flow and reached the sensor shown in Fig.5(b). Moreover, it was confirmed that the concentration ratio around the sensor was between 0.95 and 0.99.

## 3. $CO_2$ gas sensor

For the formation flight with four drones, the requirements of $CO_2$ gas sensor are lightweight (100 g or less) and wireless communication function. As a sensor with satisfying the above requirements, we selected the RICOH EH $CO_2$ sensor D101 [16] as shown in Fig.6. Figures 6(a) and 6(b) show the surface side with wireless communication using the solar panel and the protective housing, and reverse side with four intake ports (No.1-4) and two exhaust ports (No.5,6). Figure 6(c) shows the inner configuration using NDIR (Non Dispersive IfraRed)-type. The $CO_2$ concentration was calculated from Eq. (1).

$$T = \frac{I}{I_0} = e^{-\varepsilon C d} \tag{1}$$

where $T$, $I$, $I_0$, $\varepsilon$, C, and $d$ represent transmittance, intensity of transmitted light, intensity of incident light, absorbance, $CO_2$ concentration, and optical path length, respectively.

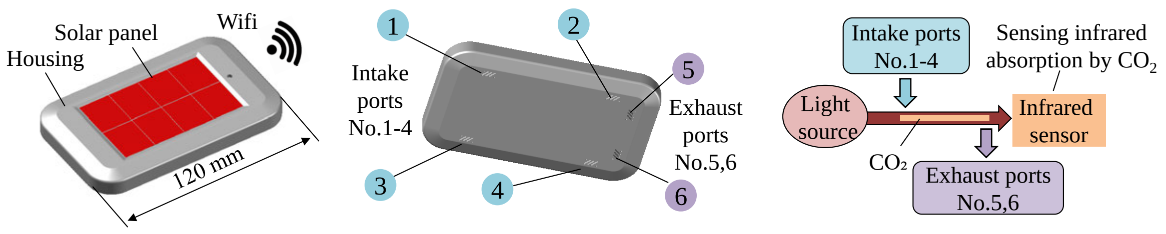


(a) Surface side　　(b) Reverse side　　(c) Inner configuration

Fig.6　Schematic of $CO_2$ sensor module and inner configuration.

## 4. Design of formation flight configuration

Figure 7 shows a schematic of formation flight configuration with four drones and the control method. The drone used was a Tello EDU with specifications listed in Table 2. The four drones were simultaneously controlled by a single personal computer using Python program. A rope was used between the connecting rod and the drone with a spacing of 1.3 m, instead of connecting the rod directly to the drone [17,18] as shown in Fig.7. With this approach, the individual differences of drone position and height were compensated for by the rope, and the formation flight with four drones were stably continued. The $CO_2$ sensor was suspended at the center of a four-drone square formation and the concentration data were sampled at 10 second intervals in the tablet computer by wireless communication function.as shown in Fig.7. The payload of a Tello EUD is 30 g as shown in Table 2. Therefore, the total payload of the formation flight with four drones becomes 120 g, and the total components weight was 111 g less than the required 120 g with the weight breakdown of components listed in Table 3.

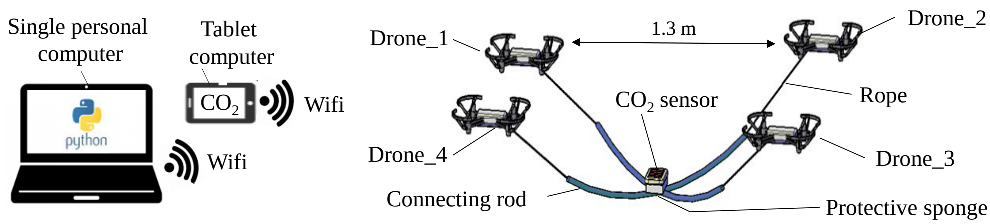


Fig.7　Schematic of formation flight configuration with four drones and the control method.

Table 2　Specifications of a drone.

| Drone | Tello EDU |
|---|---|
| Payload of a drone (g) | 30 |
| Weight (g) | 87 |
| Maximum flight time (min) | 13 |
| Number of formation flights | 4 |

Table 3　Weight breakdown of components.

| Component | Number | Weight [g] |
|---|---|---|
| Connecting rod | 4 | 16 |
| Protective sponge | 1 | 1 |
| $CO_2$ sensor | 1 | 90 |
| Rope | 4 | 4 |
| Total weight (g) | - | 111 < 120 |

## 5. $CO_2$ gas sensing experiment at the fixed position

Figure 8 shows a schematic of $CO_2$ sensing experiment at the fixed position. The $CO_2$ gas was generated by placing 400 g of dry ice in 300 g of water (mass ratio 4:3) into a plastic container with the size of 220 × 170 × 50 mm as the $CO_2$ gas source. The $CO_2$ gas source concentration was measured to be between 2,200 and 2,300 ppm by sensor. The four-drone formation hovered so that the height of $CO_2$ sensor kept 0.3 m, and the plastic container of $CO_2$ gas source was in at 5 seconds and out at 90 seconds under the four-drone formation as shown in Fig.8.

The initial indoor concentration was approximately 1,000 ppm. **Figure 9** shows the sensing results of $CO_2$ concentration for 160 seconds. When the four-drone formation was fixed in hovering mode directly above the dry ice source at a height of 0.3 m. In 5 seconds, the plastic container of $CO_2$ gas source was in under the four-drone formation. In 55 seconds, the maximum concentration of 2,100 ppm was observed corresponding to an increase of approximately 1,100 ppm over the background concentration. Moreover, in 90 seconds, the plastic container of $CO_2$ gas source was out, and in 160 seconds, $CO_2$ concentration returned to initial value as shown in **Fig.9**.

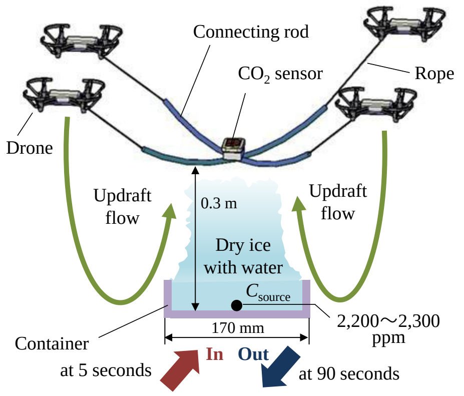


**Fig.8** Schematic of $CO_2$ sensing experiment at the fixed position.

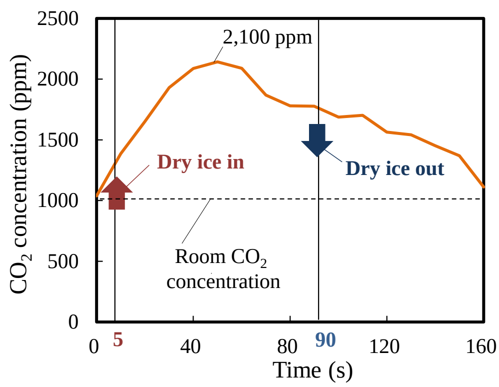


**Fig.9** Sensing results of $CO_2$ concentration.

## 6. $CO_2$ gas sensing experiment with the horizontal flight

**Figure 10** shows a schematic of $CO_2$ sensing experiment with the horizontal flight. The $CO_2$ gas was generated by placing 1,600 g of dry ice in 1,200 g of water (mass ratio 4:3) into four plastic containers with the size of 220×170×50 mm as the $CO_2$ gas source. The $CO_2$ gas source concentration was measured to be between 4,700 and 4,800 ppm by sensor as shown in **Fig.10**.

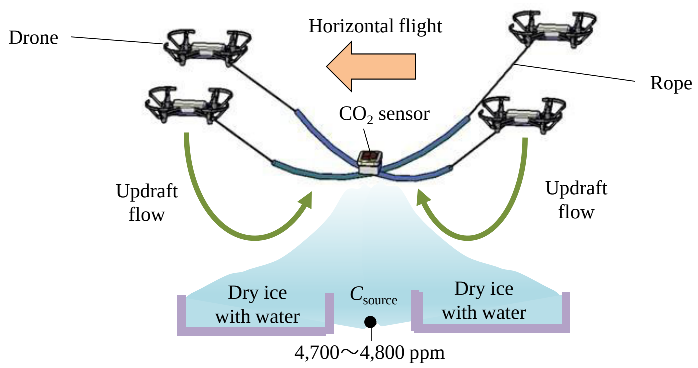


**Fig.10** Schematic of experiment with the horizontal flight.

The experiment was conducted three times, and the amount of dry ice decreased over time. Therefore, dry ice was added as needed to ensure the concentration was within the range of 4,700 to 4,800 ppm before the experiment was conducted. Additionally, experiments were conducted at two heights of 0.3 m and 0.5 m. By using Python-based automatic flight control, a flight sequence consisting of takeoff, horizontal movement, hovering for 10 seconds above the $CO_2$ source, retreat, and landing. The influence of horizontal movement on the updraft flow behavior of the formation was evaluated.

**Figure 11** shows photographs of $CO_2$ sensing experiment with the horizontal flight. **Figure 11(a)** shows flight at the height of 0.5 m, and **Figure 11(b)** shows flight at the height of 0.3 m. **Figure 12** shows sensing results of the $CO_2$ concentration **Figure 12(a)** shows the $CO_2$ concentration at the height of 0.5 m, and it was confirmed that the concentration increased to a maximum of 4,230 ppm. **Figure 12(b)** shows the $CO_2$ concentration at the height of 0.3 m, and it was confirmed that the concentration increased to a maximum of 4,673 ppm. Additionally, the prediction of $CO_2$ concentration at the source based on the two sensing points is conducted in next Chapter 7.

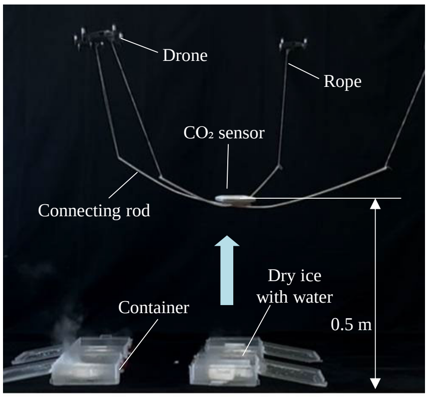


(a) Flight at the height of 0.5 m

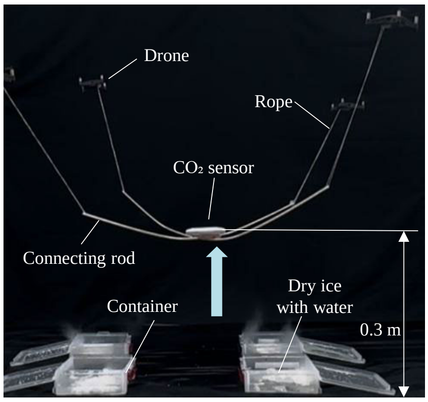


(b) Flight at the height of 0.3 m

**Fig.11** Photographs of $CO_2$ sensing experiment with the horizontal flight at the hovering for 10 seconds.

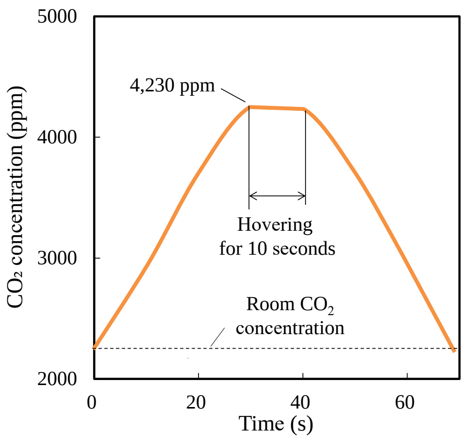


(a) Flight at the height of 0.5 m

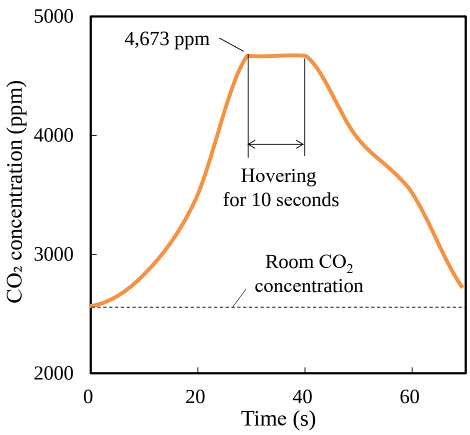


(b) Flight at the height of 0.3 m

**Fig.12** Sensing results of $CO_2$ concentration.

## 7. Prediction of $CO_2$ concentration at the source

To predict $CO_2$ concentration at the source based on the two sensing points at the heights of 0.5 m and 0.3 m, the steady-state one-dimensional convection-diffusion equation [19] is used as shown in Eq. (2).

$$u\frac{dC}{dz} = D_t\frac{d^2C}{dz^2} \tag{2}$$

where $C$, $u$, $z$, and $D_t$ represent concentration, velocity, vertical coordinates, and turbulent diffusion coefficient, respectively. Equation (2) has the exact solution with the boundary condition: $C = C_0$ at $z = 0$, $C = C_H$ at $z = H$ as shown in Eq. (3).

$$C(z) = C_0 + \frac{e^{Pe\frac{z}{H}}-1}{e^{Pe}-1}(C_H - C_0) \tag{3}$$

Here, $Pe$ is Peclet number defined as Eq. (4) using turbulent diffusion coefficient $D_t$.

$$Pe = \frac{uH}{D_t} \tag{4}$$

Table 4 shows the values for calculation of Peclet number $Pe$, we used $CO_2$ molecular diffusion coefficient $D_m = 1.64 \times 10^{-5}$ $m^2/s$ [20], and ratio of turbulent to molecular diffusion coefficient $D_t / D_m = 10^4$ (Average of $10^3$–$10^5$) [21].

Table 4 Values for calculation of Peclet number $Pe$.

| $CO_2$ molecular diffusion coefficient [20] $D_m$ ($m^2/s$) | Ratio of turbulent to molecular diffusion coefficient [21] $D_t / D_m$ | Velocity $u$ (m/s) | Height $H$ (m) |
|---|---|---|---|
| $1.64 \times 10^{-5}$ | $10^4$ (Average of $10^3$ – $10^5$) | 2.0 | 0.5 |

Table 5 shows the predicted result of concentration at the $CO_2$ source. The average concentration values of 4,290 and 4,710 ppm of three experiments ($N = 3$) were used at the heights of 0.5 m and 0.3 m, respectively. By substituting these average concentrations into Eqs. (3) and (4), the concentration at the $CO_2$ source was predicted as 4,772 ppm. Additionally, it was found that the predicted concentration of 4,772 ppm at the $CO_2$ source was in between 4,700 and 4,800 ppm measured by sensor as shown in Fig.12. Finally, the effectiveness of prediction was confirmed.

Table 5 Predicted result of concentration at the $CO_2$ source in case of horizontal fight experiment (Fig.12).

| Height (m) | Concentration (ppm) | Method |
|---|---|---|
| 0.5 | 4,290 | Experimental average $N = 3$ |
| 0.3 | 4,710 | Experimental average $N = 3$ |
| 0.0 ($CO_2$ source) | 4,772 | Using Eqs. (3) and (4) |

## 8. Discussion

It is necessary for gas sensing using drones to consider the drone down's wash flow. Therefore, there are four categories based on the amount of gas generation and the specific gravity relative to air. First category is the gas lighter than air and small amount. Second category is the gas lighter than air and large amount. Third category is the gas heavier than air and small amount. Fourth category is the gas heavier than air and large amount. Here, the determination whether to the large or small amount is based on the following criteria, that is, the large amount is defined as that the stable gas supply is larger than the blowing away by the drone's downwash.

This study belongs to fourth category, and we need to generate the updraft flow for sensing the gas heavier than air and large amount. In contrast, in case of first and third categories, the sensor must be suspended using a sufficiently long rope to avoid the influence of the flying drone's downwash. Additionally, in case of second category, the regular drone equipped with sensor can land on the gas source and sense the gas because the gas is lighter than air and large amount. To conduct the study in the above categories, it is necessary to solve the distance reached by the drone's downwash using flow simulation. We have already conducted the above study and plan to report in next paper.

## 9. Conclusion

In this study, as part of expanding drone applications, we tried to develop the $CO_2$ gas sensing method using formation flight with four drones. Flow simulation of the gas updraft flow, the construction of formation flight, $CO_2$ sensing experiments, and prediction of $CO_2$ concentration at the source were conducted. The following conclusions were obtained.

(1) By flow simulation, we confirmed the gas updraft flow not only velocity but also concentration distribution generated by the drones. It was confirmed that the updraft flow velocity around the sensor was 2 m/s at the height of 0.3 m, and the concentration ratio was between 0.95 and 0.99, respectively.
(2) A rope was used between the connecting rod and the drone, instead of connecting the rod directly to the drone. With this approach, the individual differences of drone position and height were compensated for by the rope, and the formation flight with four drones were stably continued. Then, the $CO_2$ sensing experiment using this approach was conducted. The average concentration values of 4,290 and 4,710 ppm of three experiments were measured at the heights of 0.5 m and 0.3 m, respectively.
(3) Moreover, prediction of the concentration at the $CO_2$ source was conducted using the steady-state one-dimensional convection-diffusion equation. It was found that the predicted concentration of 4,772 ppm at the $CO_2$ source was in between 4,700 and 4,800 ppm measured by sensor. Finally, the effectiveness of prediction was confirmed.

Received: December 8, 2025
Accepted: January 7, 2026

### References

[1] Li, Y., Huang, Y. and Chen, S.: "Air Quality Detection Drone System Based on Beidou Navigation System," *Computer Science and Application*, Vol. 9, No. 4, Article ID: 29659, pp. 703–709, 2019.
[2] Motlagh, N.H., Kortoçi, P., Su, X. and Lovén, L.: "Unmanned Aerial Vehicles for Air Pollution Monitoring: A Survey," *IEEE Internet of Things Journal*, Vol. 10, No. 24, pp. 21687–21704, 2023.
[3] Neumann, P.P., Hernandez Bennetts, V., Lilienthal, A.J., Bartholmai, M. and Schiller, J.H.: "Gas source localization with a micro-drone using bio-inspired and particle filter-based algorithms," *Adv. Robot.*, Vol. 27, pp. 725–738, 2012.
[4] Golston, L.M., Aubut, N.F., Frish, M.B., Yang, S., Talbot, R.W., Gretencord, C., McSpiritt, J. and Zondlo, M.A.: "Natural gas fugitive leak detection using an unmanned aerial vehicle: Localization and quantification of emission rate," *Atmosphere*, Vol. 9, No. 333. pp. 1–17, 2018.
[5] Neumann, P.P., Asadi, S., Lilienthal, A.J., Bartholmai, M. and Schiller, J.H.: "Autonomous gas-sensitive microdrone: Wind vector estimation and gas distribution mapping," *IEEE Robot. Autom. Mag.*, Vol. 19, pp. 50–61, 2012.
[6] Sato, R., Tanaka, K., Ishida, H., Koguchi, S., Ramirez., J. P. R., Matsukura, H. and Ishida, H.: "Detection of Gas Drifting Near the Ground by Drone Hovering Over: Using Airflow Generated by Two Connected Quadcopters," *Sensors*, Vol. 20, No. 5, pp. 1–16, 2020.
[7] Li, Q., Page, G.J. and McGuirk, J.J.: "Large-eddy simulation of twin impinging jets in cross-flow," *Aeronaut. J.* Vol. 111, pp.195–206, 2007.
[8] Akaogi, D., Yamashita, K., Matsukura, H., and Ishida, H.: "Development of Gas Sensing Drone: Influence of Tilted Ground on

Gas Transport," *Proc. of The Japan Society of Mechanical Engineers*, S115-05, 2021.

[9] Minamoto, Y.: "Numerical Thermo-Fluid Dynamics with Fluid Simulation Software Course Flowsquare$^+$ (1)," *Journal of Mechanical Research*, Vol. 72, No. 9, pp. 677–681, 2020.

[10] Trájer, A. J.: "Ecological evaluation of the development of Neanderthal niche exploitation," *Quaternary Science Reviews*, Vol. 310, 108127, 2023.

[11] Tajima, Y., Hiraguri, T., Matsuda, T., Imai, T., Hirokawa, J., Shimizu, H., Kimura, T. and Maruta, K.: "Analysis of Wind Effect on Drone Relay Communications," *Drones* Vol. 7, No. 3, 182, https://doi.org/10.3390/drones7030182, 2023.

[12] Togashi, S., Zhang, H. and Miyake, R.: "Development of a measuring system for the volatilization characteristics of essential oils and evaluation of the measured data by advection–diffusion simulation," *Japan Journal of Aromatherapy*, Vol. 26, No. 1, pp. 1–9, 2025.

[13] Ishigaki, Y., Kawauchi, Y., Yokogawa, S., Saito, A., Kitamura, H. and Moritake, T.: "Ventilatory effects of excessive plastic sheeting on the formation of SARS-Cov-2 in a closed indoor environment," *Environmental and Occupational Health Practice*, 5: eohp.2022-0024-OA, pp. 1–9, 2023.

[14] Koyama, S.: "Large eddy simulation of the turbulent pipe flow using dynamic subgrid-scale model," *Institute of Industrial Science*, Vol. 57, No. 1, pp. 58–62, 2005.

[15] Fujiwara, S.: "Experimental Study on Synchronized Swimming in the Kármán Vortex Behind an Object Using a Fish Robot," *Journal of Aero Aqua Bio-mechanisms*, Vol. 11, No. 1, pp. 10–17, 2025.

[16] Takeuchi, K.: "Current status and future of energy harvesting technologies," *Journal of the Japan Society for Precision Engineering*, Vol. 88, No. 11, pp. 805–808, 2022.

[17] Ando, T. and Togashi, S.: "Flight Stability Analysis of Formation Drones and Application to Netting Operation," *Technical Journal of Advanced Mobility*, Vol. 6, No. 8, pp. 57–66, 2025.

[18] Ando, T., Aoki, H. and Togashi, S.: "Flight Stabilization of Drones near Ceiling and Its Application to Cabling," *Proc. of the 30th Annual Meeting of Kanto Branch*, JSME, 14G02, 2024.

[19] Ferziger, J. and Peric, M.: Computational method for fluid dynamics, 3rd Edition, Springer, pp. 76–83, 2002.

[20] Matsunaga, N., Hori, M. and Nagashima, A.: "5th Report Measurements of the mutual diffusion coefficients of gases by the Taylor method," *Transactions of the Japan Society of Mechanical Engineers.* Part B, Vol. 64; No. 621, pp. 149–155, 1998.

[21] Levenspiel, O.: Chemical Reaction Engineering, 3rd ed., John Wiley & Sons, p. 311, 1999.

**張　　山峰**
2025年3月国士舘大学理工学部機械工学系卒業。富樫研究室に所属時に編隊飛行する4台のドローンによる$CO_2$検知法を開発し，Technical Journal of Advanced Mobility ポスターセッション in Japan Drone 2025 に発表。2025年4月早稲田大学大学院生命理工専攻に進学。現在，介護分野へのセンシング技術の応用拡大に取り組んでいる。
E-mail：zsf@akane.waseda.ac.jp

**富樫　盛典**
1995年3月東京大学大学院工学系研究科機械工学専攻博士課程修了，博士（工学）。1995年4月（株）日立製作所機械研究所に入社。研究室長，主管研究員を歴任。日本機械学会フェロー，日本流体力学会フェロー。2020年4月より国士舘大学理工学部機械工学系の教授として着任。流体力学的観点からドローンの適用拡大の研究を推進中。JUIDA 無人航空機操縦士，一等無人航空機操縦士（国家資格）。
E-mail：togashis@kokushikan.ac.jp

**吉村　越輝**
2022年4月国士舘大学理工学部機械工学系入学。富樫研究室に所属。流体力学的観点からドローンの適用拡大の研究を推進中。主に，ドローンによる$CO_2$検知法，飛行しているドローンからの流体音による状態診断の開発に取り組んでいる。
E-mail：s23a362b@kokushikan.ac.jp

## 一般社団法人 日本 UAS 産業振興協議会（JUIDA）

JUIDA は、日本の無人航空機システム（UAS）の、民生分野における積極的な利活用を推進し、UAS 関係の新たな産業・市場の創造を行うとともに、UAS の健全な発展に寄与することを目的とした中立、非営利法人として、2014 年 7 月に設立されました。

国内外の研究機関、団体、関係企業と広く連携を図り、UAS に関する最新情報を提供するとともに、さまざまな民生分野に最適な UAS を開発できるような支援を行っています。同時に、UAS が安全で、社会的に許容されうる利用を実現するために、操縦技術、機体技術、管理体制、運用ルール等の研究を行うとともに政策提言を行っています。

**Technical Journal of Advanced Mobility**
**次世代移動体技術誌**

**第 7 号**

発行日　：2026 年 1 月 20 日
編集・発行　：一般社団法人日本 UAS 産業振興協議会
東京都文京区本郷 5-33-10
いちご本郷ビル 4F
URL　：https://uas-japan.org/
email　：journal@uas-japan.org



ISSN　2435-5453